MedChemComm

Accepted Manuscript

This is an *Accepted Manuscript*, which has been through the Royal Society of Chemistry peer review process and has been accepted for publication.

Accepted Manuscripts are published online shortly after acceptance, before technical editing, formatting and proof reading. Using this free service, authors can make their results available to the community, in citable form, before we publish the edited article. We will replace this *Accepted Manuscript* with the edited and formatted *Advance Article* as soon as it is available.

You can find more information about *Accepted Manuscripts* in the Information for Authors.

Please note that technical editing may introduce minor changes to the text and/or graphics, which may alter content. The journal's standard Terms & Conditions and the Ethical guidelines still apply. In no event shall the Royal Society of Chemistry be held responsible for any errors or omissions in this *Accepted Manuscript* or any consequences arising from the use of any information it contains.

ROYAL SOCIETY OF CHEMISTRY

www.rsc.org/medchemcomm

Design, synthesis and evaluation of novel π-π stacking nano-intercalator as anti-tumor agent[†]

Haimei Zhu,[a‡] Yuanbo Song,[c‡] Yuji Wang, [a] Ming Zhao,[a,b]* Yi Ren,[a] Yaonan Wang,[a] Shurui Zhao,[a] Jianhui Wu,[a] Shiqi Peng[a]*

[a]Beijing area major laboratory of peptide and small molecular drugs; Engineering Research Center of Endogenous Prophylactic of Ministry of Education of China; Beijing Laboratory of Biomedical Materials; College of Pharmaceutical Sciences, of Capital Medical University, Beijing 100069, China; E-mail: sqpeng@bjmu.edu.cn

[b]Faculty of Biomedical Science and Environmental Biology, Kaohsiung Medical University, Kaohsiung, Taiwan

[c]Guangxi Pusen Biotechnology Co. ltd.

*To whom correspondence should be addressed. E-mails: sqpeng@bjmu.edu.cn and mingzhao@bjmu.edu.cn.

‡ These authors contributed equally.

† The authors declare no competing interests.

Abstract

Based on the knowledge that cyclohexane-1,4-dione, piperazine and β-carboline are the essential building blocks of DNA intercalators, β-carboline-3-carboxylic acid is a π-π stacking like DNA intercalator, and β-carboline derivatives can form nanoparticles, this paper hypothesized that (2'*S*,5'*S*)-tetrahydropyrazino[1',2':1,6]-di{2,3,4,9-tetra-hydro-1*H*-pyrido[3,4-b]indole}-1',4'-dione (THPDTPI) would be a π-π stacking lead nano-intercalator. The docking investigation explored that THPDTPI can intercalate into DNA with a π-π stacking manner. The simple condensation of 3S-1,2,3,4-tetra-hydro-β-carboline-3-carboxylic acid provided THPDTPI in good yield and high purity. The TEM, SEM and AFM imaging visualized that THPDTPI formed nanoparticles in ultrapure water, in solid state and in rat plasma. Faraday-Tyndall effect proved that THPDTPI exhibited nano-properties in pH 2.0 and pH 7.0 water. Spectrophotometric assays suggested that the interaction model of THPDTPI and CT DNA was π-π stacking intercalation. *In vivo* THPDTPI dose-dependently slowed the tumor growth of S180 mice with a minimal effective dose of 0.01 μmol/kg/day. *In vitro* THPDTPI exhibited anti-proliferation activities on S180 and Hela cells with IC_{50} values of 0.39 and 3.5 μM, respectively. Even when the single dose was raised up to 10000 folds of the minimal effective dose, i.e. 100μmol/kg, THPDTPI still did not show liver, kidney and systematic toxicity in mice. These findings provide a strategy for designing THPDTPI like π-π stacking nano-intercalators.

Keywords: π-π stacking, intercalation, nanoparticles, anti-tumor, toxicity.

Introduction

DNA is an inarguably indispensable target for developing anti-cancer drugs. The constant struggle of developing potent anticancer drugs leads to the discovery of a series of DNA binding lead compounds such as amino substituted benzimidazo-[1,2-*a*]quinolines,[1] 3-formylchromones,[2] 9-aminoacridine and proflavine,[3] carbazole-pyrrolo[2,1-*c*][1,4]-benzodiazepine conjugates,[4] aa-Trp-Trp-OBzls,[5] acenaphtho[1,2-*b*]pyrroles,[6] ethidium bromide and 4-methyl-2,7-diamino-5,10-diphenyl-4,9-diazapyrenium hydrogensulfate,[7] five and six member ring dual DNA intercalators,[8] triplex-selective indoloquinolines,[9] conjugates of β-carboline with chalcone,[10] 1,2,3-triazol-1,8-naphthalimides,[11] mono- and bis-phenothiaziniumepiperazin-exylene,[12] nitroacridines, thienoquinolone, cumoestrol, mitoxantrone, daidzein and genistein,[13] bis-ethidium and bis-acridine,[14] acridine-3-carboxamides and acridine-4-carboxamides,[15] and N-(3-benzyloxycarbonylcarboline-1-yl)ethylamino acid benzylesters.[16] These lead compounds are capable of targeting DNA either via groove binding or via intercalation, of which piperazine, cyclohexane-1,4-dione and β-carboline are the interesting building blocks. It is well documented that the groove binding determines little perturbations of the B-form DNA double helix, but *via* π-π stacking the intercalation can lead the paired DNA bases to an unwinding status and consequently can overcome resistance phenomena common to other anti-cancer drugs.[17,18,19] It is also well documented that π-π stacking is a key step to DNA intercalating mechanism of β-carbolines.[20] These knowledge emphasize that the discovery of novel π-π stacking nano-intercators is of chemotherapeutic importance.

In view of structural impression of piperazine, β-carboline and cyclohexane-1,4-dione, a novel heterocycle, (2'*S*,5'*S*)-tetrahydropyrazino[1',2':1,6]-di{2,3,4,9-tetrahydro-1*H*-pyrido[3,4-b]indole}-1',4'-dione (THPDTPI) was constructed and the design is graphically illustrated with Scheme 1. To the best of our knowledge, THPDTPI would be a nano-medicine capable of targeting DNA.[21,22] The present paper calculated the docking energy of THPDTPI towards the double strand B-form DNA to predict its potential target, discussed its synthesis, visualized its nano-structure, evidenced

physical and chemical mechanism of it intercalating DNA, evaluated its anti-tumor activity *in vitro* and *in vivo*, and explored its liver and kidney toxicity.

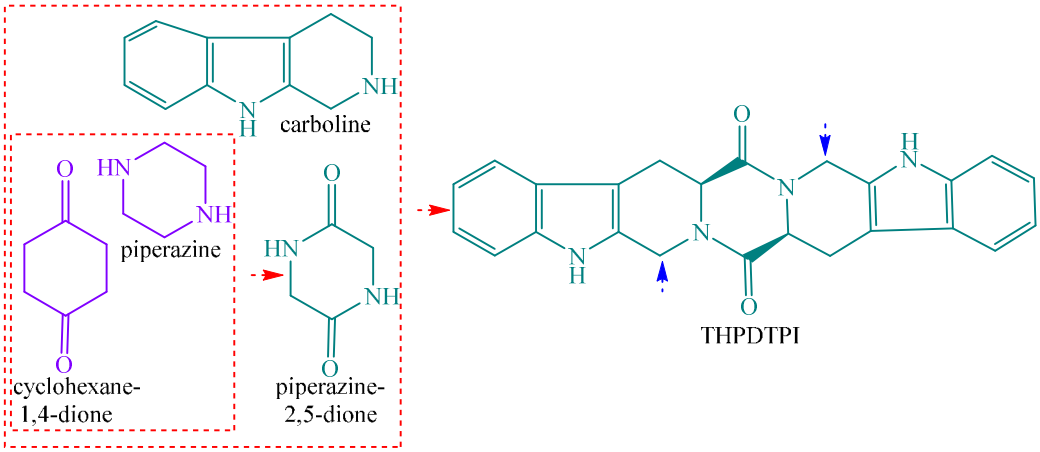

Scheme 1 Design of novel DNA intercalator, heterocycle THPDTPI, wherein the blue arrowheads represents the easy modifying positions.

Results and discussion

Docking of THPDTPI towards double strands B-form DNA

The rationality of the design and the intercalation model were examined with docking investigation. Fig. 1 shows that THPDTPI intercalates into the bases of double strands B-form DNA with a typical π-π stacking manner. The carboline moieties of THPDTPI properly approach the two base pairs of DNA. Here this proximity is illustrated with the distances between 13 atoms of the carboline moieties and 23 atoms of two purine/pyrimidine pairs, which ranged from 3.0 Å to 3.9 Å, and marked with the green solid lines. This proximity also results in two hydrogen bond interactions between the two hydrogens of the pyrroles of THPDTPI and the two oxygens of the phosphate (1.9 Å) and the deoxyribose (2.2 Å) of DNA, and marked with green dashed lines. Reasonably, the hydrogen bonds can stabilize the π-π stacking. On the other hand, the free energy of THPDTPI binding DNA is -9.32 kcal/mol.

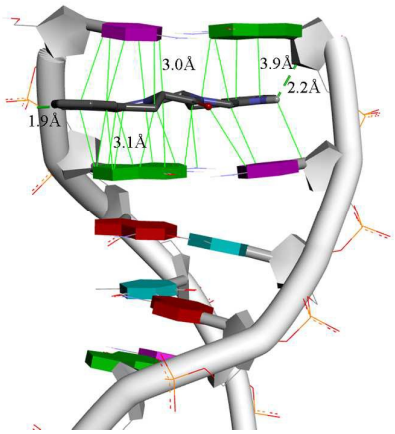

Fig. 1 Docking of THPDTPI towards the double strands B-from DNA. THPDTPI is represented in stick model, hydrogen bonds are represented with green dashed lines, while the π-π stacking and distances between THPDTPI and DNA bases are represented with green solid lines.

Synthetic route of preparing THPDTPI

THPDTPI was prepared according to a synthetic route depicted in Scheme 2, in which two cyclizations were involved. Firstly the Pictet-Spengler cyclization resulted in 3S-1,2,3,4-tetrahydro-β-carboline-3-carboxylic acid, and secondly the intermolecular cyclization provided THPDTPI. The detailed preparation was described in the following synthetic procedure.

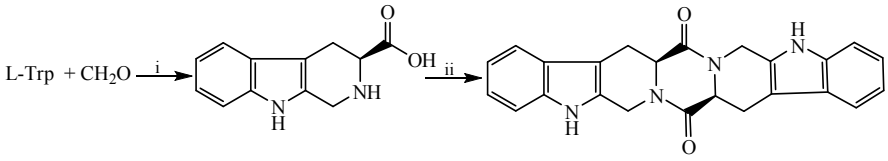

Scheme 2 Synthetic route of the preparation of THPDTPI. i) Sulfuric acid (1 M); ii) EDC, N-hydroxybenzotriazol, DMF, N-methylmorpholine.

Synthetic procedures of THPDTPI

Preparing 3S-1,2,3,4-tetrahydro-β-carboline-3-carboxylic acid

To a mixture of 5.0 g (24.5 mmol) of L-Trp, 25 mL of H_2SO_4 (1 M) and 80 mL of water, 8 mL of formaldehyde (36-38%) were added. The reaction mixture was stirred at room temperature for 2 h and adjusted to pH 7 with concentrated ammonia liquor. The mixture was kept at 0 ºC for 12 h, and the formed precipitates were collected by filtration. The recrystallization gave 3.97 g (75%) of the title compound as colorless powders. Mp 280-282 ºC and the structure was confirmed with spectra. ESI/MS: 217 $[M + H]^+$. IR (KBr): 3450, 3200, 3000, 2950, 2850, 1700, 1601, 1452, 1070, 900 cm^{-1}.

^{1}HNMR (BHSC-500, DMSO-d6): δ=10.99 (s, 1H), 9.89 (s, 1 H), 7.30 (t, *J*=7.5 Hz, 1H), 7.22 (t, *J*=8.0 Hz, 1 H), 7.01 (d, *J*=8.0 Hz, 1 H), 6.81 (d, *J*=7.5 Hz, 1 H), 4.01 (t, *J*=4.8Hz, 1H), 3.75 (dd, *J*=10.5 Hz, *J*=5.0 Hz, 1 H), 3.64 (dd, *J*=10.5 Hz, *J*=2.4 Hz, 1 H), 2.91 (d, *J*=10.5 Hz, 2 H), 2.86 (s, 1 H).

Preparing THPDTPI

To a mixture of 648 mg (3 mmol) of 3S-1,2,3,4-tetrahydro-β-carboline-3-carboxylic acid, a solution of 573 mg (3 mmol) of EDC and 405 mg (3 mmol) of N-hydroxybenzotriazol in 20 mL of anhydrous N,N-dimethylformamide was added. The reaction mixture was adjusted to pH 9 by adding 0.3 mL of N-methylmorpholine and then was stirred at room temperature for 12 h. TLC (CH_2Cl_2/CH_3OH, 15/1) indicated the reaction was completed. At 45 °C the reaction mixture was evaporated under vacuum. The residue was successively triturated with water and acetone, and then purified on silica gel column (CH_2Cl_2/CH_3OH, 30/1) to provide 535 mg (90%) of the title compound as colorless powders, of which the structure was confirmed with spectra. FT-MS 397.1586 $[M + H]^+$. ^{1}H NMR (800 MHz, $CDCl_3$): δ=7.930 (s, 2H), 7.448 (d, *J*=8.0 Hz, 2H), 7.360 (d, *J*=8.0 Hz, 2H), 7.204 (t, *J*=8.0 Hz, 2H), 7.124 (t, *J*=8.0 Hz, 2H), 5.737 (d, *J*=16.0 Hz, 2H), 4.468 (dd, *J*=12.0 Hz, *J*=4.0 Hz, 2H), 4.264 (d, *J*=16.0 Hz, 2H), 3.535 (dd, *J*=14.4 Hz, *J*=2.4 Hz, 2H), 2.927 (t, *J*=13.6 Hz, 2H). ^{13}C NMR (125 MHz, DMSO-d6): δ=169.98, 165.05, 136.71, 136.46, 130.31, 128.40, 126.75, 121.72, 121.60, 119.22, 118.24, 118.15, 111.63, 107.11, 106.01, 57.06, 56.46, 40.97, 28.06, 23.44.

HPLC purity of THPDTPI

By following the methods in ESI† the chromatogram was recorded, a sole peak of THPDTPI occurred at 5.704 minutes and the relative area of the peak was 98.9%. Therefore the retention time of THPDTPI is 5.704 minutes and the HPLC purity of THPDTPI is 98.9%.

FT-MS spectrum and THPDTPI forming dimer

Mass spectrum was measured on a SolariX FT-ICR mass spectrometer (Bruker Daltonics) with ESI negative ion source and superconductive magnet of 9.4 T. Fig. 2A shows the spectrum of 1 nM solution of THPDTPI in ultrapure water, gives a

negative ion peak at 827.28939, the mass of a dimer plus Cl, and gives a negative ion peak at 431.12884, the mass of monomer plus Cl. Since Fig. 2A is a qCID spectrum the monomer is the fragmentation product of the dimer, and the dimer is the unified form of the existence of THPDTPI in ultrapure water. The full mass spectrum is given in ESI.†

NOESY 2D NMR and four interesting cross-peaks

To reveal the manner of the dimerization the NOESY 2D NMR was measured on 800 MHz in deuterated DMSO. Fig. 2B shows NOESY 2D ^{1}HNMR spectrum of THPDTPI, in which four interesting cross-peaks are marked with red circles. Cross-peak 1 mirrors the interactions between the pyrrole H of the carboline moiety of one molecule with the H at the 1-position of the carboline moiety of another molecule. Cross-peak 2 mirrors the interactions between the H at 7,8-positions of the carboline moiety of one molecule with the pyrrole H of the carboline moiety of another molecule. Cross-peaks 3 and 4 mirror the interactions between the H at 7 and 8-positions of the carboline moiety of one molecule with the H at 4-position of the carboline moiety of another molecule. All the NMR spectra are also given in the ESI.†

Energy minimized conformation based dimer

To visualize the dimer, THPDTPI was sketched in ChemDraw 10.0, converted to 3D conformation in Chem3D 10.0, and then energy minimized in Discovery Studio 3.5 with a Merck molecular force field (Merck & Co.). Energy-minimized conformation was utilized to form a dimer. Fig. 2C and 2D indicate that to match the requirements of the 4 interesting cross-peaks of Fig. 2B the two energy-minimized conformations of THPDTPI have to approach in a typical π-π stacking manner. NOESY 2D ^{1}HNMR experiment, therefore, implies that the π-π stacking should be an essential manner of THPDTPI intercalating DNA.

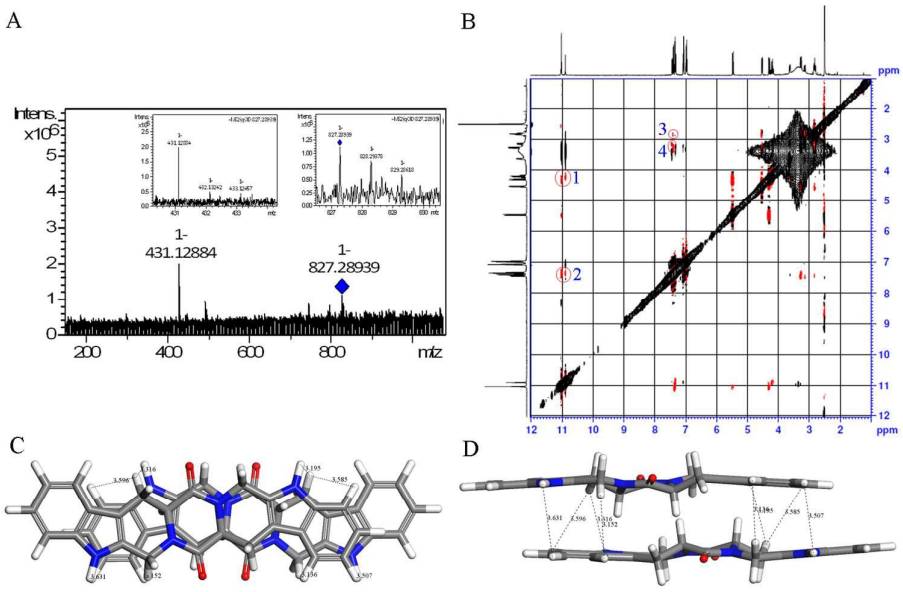

Fig. 2 FT-MS and NOESY 2D ^{1}HNMR spectra of THPDTPI, (A) qCID spectrum of 1 nM solution of THPDTPI in ultrapure water; (B) NOESY 2D ^{1}HNMR spectrum of THPDTPI and 4 interesting cross-peaks; (C) Top view of 2 molecules of THPDTPI approaching in π-π stacking manner; (D) Front view of 2 molecules of THPDTPI approaching in π-π stacking manner.

Faraday-Tyndall effect and nano-properties of THPDTPI in water

To explore the nano-properties of the aqueous solution of THPDTPI, the laser (650 nm) induced Faraday-Tyndall effect was tested and is shown in Fig. 3. As seen, when 1 nM solution of THPDTPI in pH 2.0 and pH 7.0 ultrapure water are irradiated with 650 nm laser beam the Faraday-Tyndall effects clearly occur (Fig. 3D, E). In addition, the zeta potential and size of THPDTPI in water were determined on a Malvern's Zetasizer (Nano-ZS90; Malvern Instruments) with the DTS (Nano) Program. Fig. 3F indicates that the zeta potential of THPDTPI in pH 7.0 ultrapure water (1 nM) is -20.60 mV with 4.42 mV of half width. Fig. 3G, H indicate that the mean size of THPDTPI in pH 2.0 and pH 7.0 ultrapure water are 164.2 ± 1.91 nm and 141.8 ± 1.91 nm, respectively. Therefore, the pH 2.0 and pH 7.0 aqueous solution of THPDTPI possess nano-properties.

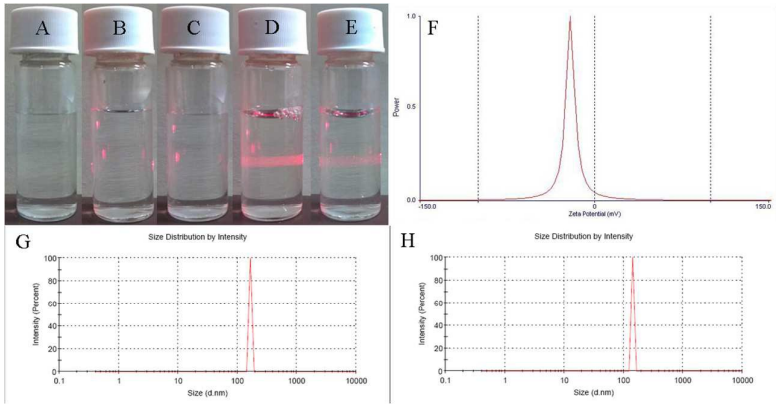

Fig. 3 Tyndall effect, zeta potential and size of THPDTPI in ultrapure water. (A) Ultrapure water no radiation; (B) pH 2.0 ultrapure water with 650 nm laser radiation; (C) pH 7.0 ultrapure water with 650 nm laser radiation; (D) 1 nM solution of THPDTPI in pH 2.0 ultrapure water with 650 nm laser radiation; (E) 1 nM solution of THPDTPI in pH 7.0 ultrapure water with 650 nm laser radiation; (F) zeta potential of 1 nM solution of THPDTPI in pH 7.0 ultrapure water; (G) size of THPDTPI in pH 2.0 ultrapure water; (H) size of THPDTPI in pH 7.0 ultrapure water.

Theoretically predicted nanoparticle size of THPDTPI

To theoretically predict the formation and the size of the nanoparticles, the mesoscale simulation software was used to perform the calculation. The molecule of THPDTPI was built and optimized in the Visualizer window. "Beads" were constructed from atomistic simulations and placed at the center-of-mass of groups of the atoms corresponding to particular parts of a molecule. Fig. 4 indicates that in a nanoparticle of 8.5 nm in diameter there are 608 molecules of THPDTPI.

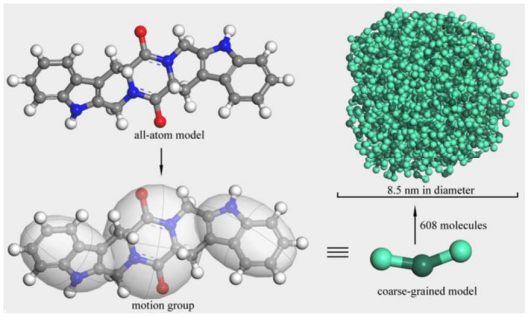

Fig. 4 Proposed model of THPDTPI forming nanoparticles.

TEM image of THPDTPI nanoparticles

The shape and size of THPDTPI in aqueous solution were imaged with transmission electron microscopy (TEM). The TEM images of THPDTPI in pH 7.0 ultrapure water (Fig. 5A-5C) indicate that in 10.0, 1.0 and 0.1 nM of solutions THPDTPI forms nano-particles of 8.5-146.5 nm, 30.2-46.5 nm and 46.5-116.3 nm in diameter, respectively.

The comparison of the diameters of the nanoparticles in three concentration solutions suggests that in 1.0 nM solution THPDTPI forms nanoparticles of the most suitable size. On the other hand, in 10.0 nM solution THPDTPI forms the nanoparticle of 8.5 nm in diameter, the smallest particle. According to theoretical prediction, this particle should contain 608 molecules of THPDTPI.

SEM image of THPDTPI nanoparticles

The shape and size of THPDTPI in solid state were imaged with scanning electron microscopy (SEM). Fig. 5D indicates that in the solid state THPDTPI exists as sphere of 2-14 μm in diameter. The amplified insert indicates that the spheres consist of the nanoparticles of ~140 nm in diameter, which are marked with red circles. Thus it could be hypothesized that during the evaporation of 10.0 nM aqueous solution of THPDTPI the smaller nanoparticles gradually aggregate and finally form the microspheres.

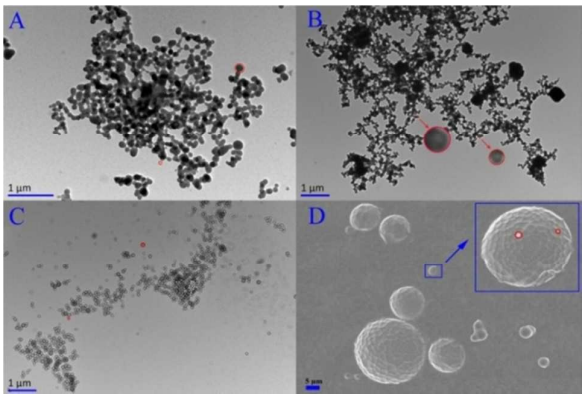

Fig. 5 TEM and SEM images of THPDTPI. (A) TEM image of THPDTPI in pH 7.0 ultrapure water (10.0 nM); (B) TEM image of THPDTPI in pH 7.0 ultrapure water (1 nM); (C) TEM image of THPDTPI in pH 7.0 ultrapure water (0.1 nM); (D) SEM image of the precipitates formed by evaporating an aqueous solution of THPDTPI in pH 7.0 ultrapure water (10.0 nM).

AFM image of THPDTPI nanoparticles

The shape and size of THPDTPI in blood were imaged with atomic force microscopy (AFM). Fig. 6A indicates that rat plasma alone gives no interesting nanoparticle. Fig. 6B-6D indicate that in 1 nM rat plasma THPDTPI forms the nanoparticles of 77.5 - 121.1 nm in height, suggesting in rat blood THPDTPI is still able to form the suitable nanoparticles for delivery in the circulation.

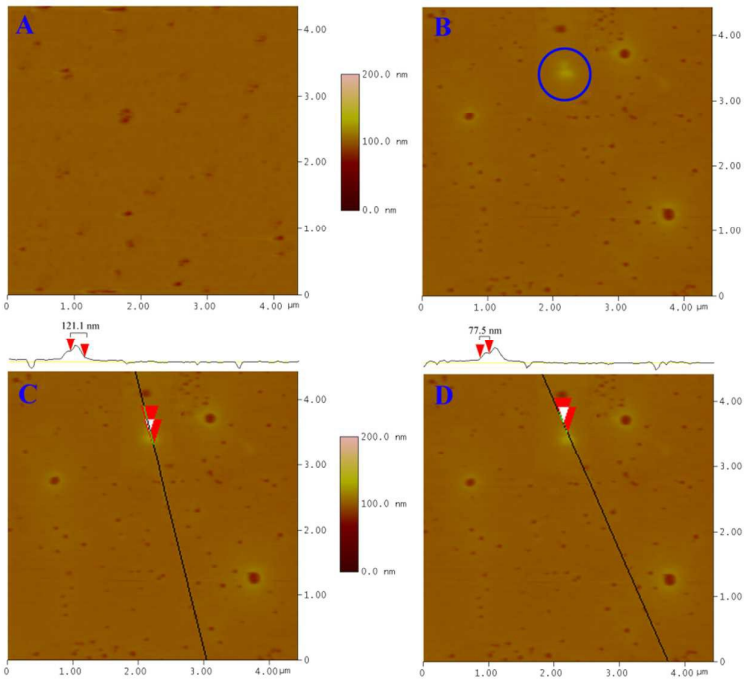

Fig. 6 AFM image of THPDTPI in rat plasma. (A) AFM image of rat plasma alone; (B) AFM image of THPDTPI in rat plasma (0.1 nM), in which two nanoparticles been marked with a blue ring; (C) scaled AFM image of the down particle inside the blue ring; (D) scaled AFM image of the up particle inside the blue ring.

Anti-tumor activity of THPDTPI *in vivo*

To show the anti-tumor activity and the dose-dependent relationship, male S180 mice were used and the assay was performed by following the standard procedure and the activity was represented with tumor weight. Fig. 7 indicates that after 14-day treatment the tumor weights of the mice orally treated with THPDTPI (0.01, 0.1 and 1.0 μmol/kg/day) are significantly lower than that of the mice treated with 0.5% carmellose sodium (CMCNa, vehicle, 0.2 mL/mouse/day), suggesting THPDTPI is an active anti-tumor agent. Beside, with the increase of the dose the tumor weight gradually decreases, suggesting THPDTPI slows the tumor growth in a dose-dependent manner. Furthermore, the tumor weight of the mice orally treated with 1 μmol/kg/day of THPDTPI is equal to that of the mice intraperitoneally treated with 2 μmol/kg/day of doxorubicin (Dox, positive control), suggesting the activity of THPDTPI is 2 folds higher than that of Dox. Therefore, in respect of anti-tumor activity and nano-property, THPDTPI is an excellent lead anti-tumor agent possessing nano-properties.

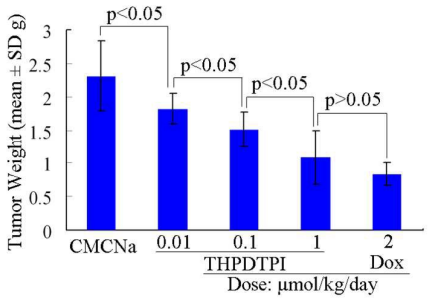

Fig. 7 Tumor weights of the S180 mice treated with various doses of THPDTPI, n=12.

Spectrophotometric assays and intercalation of THPDTPI towards CT DNA

To confirm the intercalation model of THPDTPI binding DNA, the spectrophotometric assays were performed. Fig. 8A gives increased absorption at 208 nm and 258 nm in the UV spectra of 0.9 μM THPDTPI with increased amount of CT DNA. Fig. 8B gives increased absorption at 208 nm but decreased absorption at 258 nm in the UV spectra of 200 μM CT DNA with increased amount of THPDTPI. Furthermore, Fig. 8B shows obvious red shift at 208 nm in the UV spectra while increasing the amount of THPDTPI in 200 μM CT DNA. The increased absorption at 208 nm and 258 nm in Fig. 8A and the decreased absorption at 258 nm in Fig. 8B demonstrate that CT DNA exhibits strong absorption at both 208 nm and 258 nm, while THPDTPI exhibits strong absorption at 208 nm only. The obvious red shifts at 208 nm in Fig. 8B suggests THPDTPI intercalates into CT DNA and the maximal absorption wave length of the complex drifts to 220 nm.[23,24]

Fig. 8C gives decreased fluorescence intensity at 345 nm in the fluorescence spectra of 0.18 μM THPDTPI with increased amount of CT DNA, while Fig. 8D gives increased fluorescence intensity at 345 nm in the fluorescence spectra of 80 μM CT DNA with increased amount of THPDTPI. The decreased fluorescence intensity in Fig. 8C and the increased fluorescence intensity in Fig. 8D demonstrate that THPDTPI possesses much stronger fluorescence intensity than CT DNA does at 345 nm. The quenching of THPDTPI fluorescence intensity with increasing amount of CT DNA in Fig. 8C suggests THPDTPI intercalates into CT DNA.[25]

According to a general understanding, the circular dichroism (CD) spectrum of right handed B-form DNA is characterized by its positive and negative bands, of which the former is due to base stacking and the latter is due to helicity. The spectral changes of

these two bands are usually the result of the intercalation of small molecules with CT DNA.[25] The circular dichroism (CD) spectra of 14 μM CT DNA with increasing amount of THPDTPI (Fig. 8E) exhibit decreased shift of the positive bands at 280 nm and increased shift of negative bands at 255 nm, respectively. These results suggest that the intercalation of THPDTPI into CT DNA induces constant conformational changes of CT DNA.

Fig. 8F shows the effect of increasing amounts of THPDTPI on the relative viscosity of CT DNA at 25 ± 0.1 ºC. The relative viscosity of 14 μM of CT DNA gradually increases while mixing with increased amount of THPDTPI, which suggests THPDTPI intercalates into CT DNA and the viscosity of the formed complex becomes larger than CT DNA alone.[25]

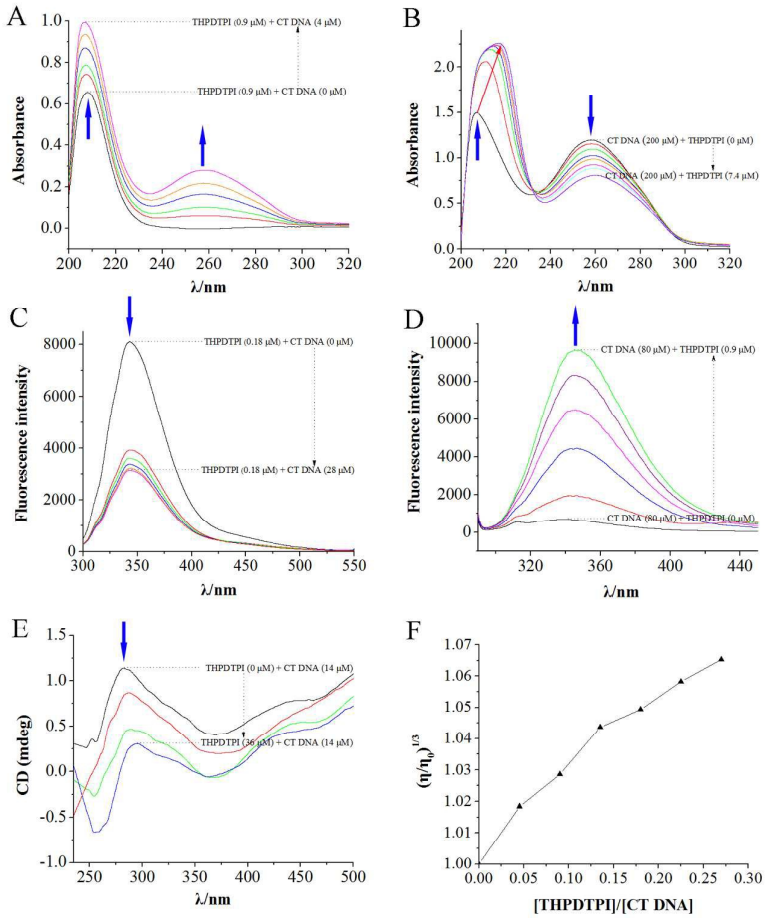

Fig. 8 Intercalation of THPDTPI towards CT DNA *in vitro*. (A) UV spectrum of 0.9 μM of THPDTPI with increased amount of CT DNA; (B) UV spectra of 200 μM of CT DNA with increased amount of THPDTPI; (C) fluorescence spectra of 0.18 μM of THPDTPI with increased

amount of CT DNA; (D) fluorescence spectra of 80 μM of CT DNA with increased amount of THPDTPI; (E) circular dichroism (CD) spectra of 14 μM of CT DNA with increased amount of THPDTPI; (F) the relative viscosity of 14 μM of CT DNA with increased amount of THPDTPI.

Anti-proliferation activity of THPDTPI *in vitro*

The *in vitro* activity of THPDTPI (final concentrations: 0.01, 0.1, 1, 5, 10 and 50 μM) inhibiting cancer cell proliferation was assayed on S180 and HeLa cells using MTT method, and represented with IC_{50} values. The concentration curves demonstrated that the IC_{50} values of THPDTPI against S180 and HeLa cells are 0.39 μM and 3.5 μM, respectively. Since THPDTPI has blue emission fluorescence, to visualize THPDTPI inside cancer cells S180 and HeLa cells were incubated with DMEM medium or 3.5 μM of THPDTPI for 24 h and the confocal images are shown in Fig. 9. As seen, no blue fluorescence can be seen inside S180 and HeLa cells incubated with DMEM medium (Fig. 9A and 9C), while obvious (Fig. 9B) and weak (Fig. 9D) blue fluorescence can be seen inside the nucleus of S180 and HeLa cells incubated with THPDTPI. These observations imply that THPDTPI inhibits the proliferation of cancer cells by entering their nucleus. Both the IC_{50} values and confocal images show that THPATPI possesses a stronger anti-proliferation activity on S180 cells than on Hela cells.

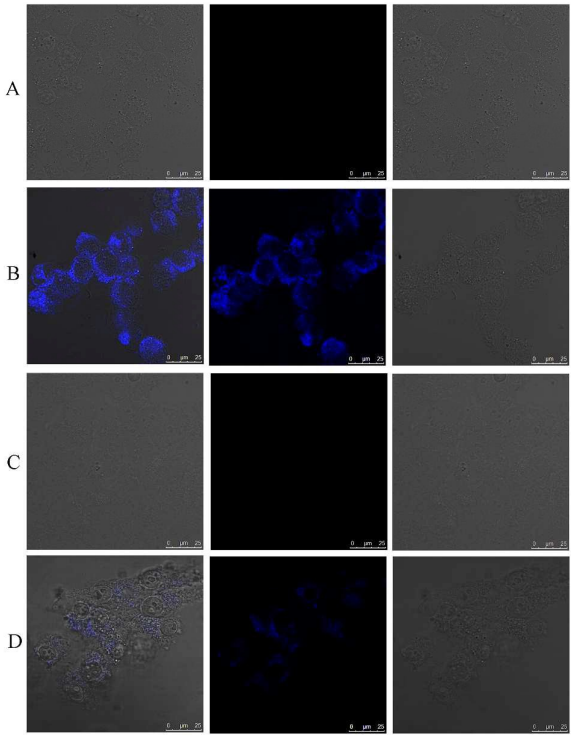

Fig. 9 Confocal images: (A) for S180 cells that incubated with DMEM medium; (B) for S180 cells that incubated with 3.5 μM of THPDTPI; (C) for HeLa cells that incubated with DMEM medium; (D) for HeLa cells that incubated with 3.5 μM of THPDTPI.

Acute toxicity of THPDTPI

To estimate the acute toxicity the healthy ICR mice were orally treated with THPDTPI at a single dose of 100 μmol/kg, a dose of 10000 times of the minimal effective dose (0.01 μmol/kg), and the mice were monitored for 7 days. Four hours after the administration the orbital blood of the mice were collected to determine the serum level of alanine transaminase (ALT), aspartate transaminase (AST) and creatinine (Cr). On 7th day the mice received ether anaesthesia and were sacrificed to sample the blood and the organs to determine serum ALT, AST and Cr, as well as to examine morphological change of the organs. Fig. 10A-10C indicates that similar to CMCNa, a single oral dose of 100 μmol/kg of THPDTPI does not change the serum ALT, AST and Cr of healthy mice, suggesting THPDTPI possesses no liver and kidney toxicity. It is also found that during 7-day observation the mice exhibit normal behavior and their organs have no morphological change, suggesting THPDTPI possesses no systematic toxicity. Besides, THPDTPI and CMCNa treated S180 mice have similar organ weight which is shown in Fig. S6 of the ESI†. This means that the administration THPDTPI induces no organ toxicity, and consequently induces no Dox-like heart toxicity in particular.

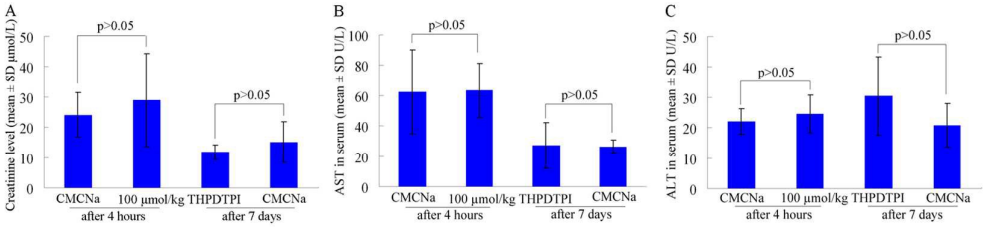

Fig. 10 Serum ALT (A), AST (B) and Cr (C) of the mice treated with 100 μmol/kg single dose of THPDTPI.

THPDTPI potentially targeting tumor tissue

To estimate the distribution of THPDTPI, the brain, heart, spleen, liver, kidney, lung, blood and tumor of the S180 mice treated with CMCNa or 1.0 μmol/kg/day of THPDTPI were homogenized, ultrasonically extracted with dichloromethane, centrifuged at 1000 g for 10 minutes to separate the supernatant for ESI(-/+)-MS tests.

It was found that ESI(-/+)-MS spectra of the extracts of the brain, heart, spleen, liver, kidney, lung and blood, but not the extracts of the tumor tissue, failed to give any ion peak relate to THPDTPI. Fig. 11A and 11C are the ESI(-/+)-MS spectra of the tumor tissue of S180 mice treated with 1.0 μmol/kg/day of THPDTPI for 7 days, while Fig. 11B and 11D are the ESI(-/+)-MS spectra of the tumor tissue of S180 mice treated with CMCNa. The ESI(+)-MS and ESI(-)-MS spectra of the extract of the tumor tissue of S180 mice treated with THPDTPI give an ion peak at 419.10190 of $[M + Na]^+$ and an ion peak at 431.09567 of $[M + Cl]^-$, respectively. The ESI(+)-MS and ESI(-)-MS spectra of the extract of the tumor tissue of S180 mice treated with CMCNa give no comparable ion peak at the corresponding area. ESI(-/+)-MS spectrum analysis suggests that THPDTPI would be a tumor targeting lead compound. It is worthy to emphasize that ESI(-/+)-MS spectra of the extract of the heart of 1.0 μmol/kg/day of THPDTPI treated S180 mice failed to give any ion peak related to THPDTPI. This means that the administration induces no accumulation of THPDTPI in the heart of the treated mice, and consequently results in no Dox-like heart toxicity.

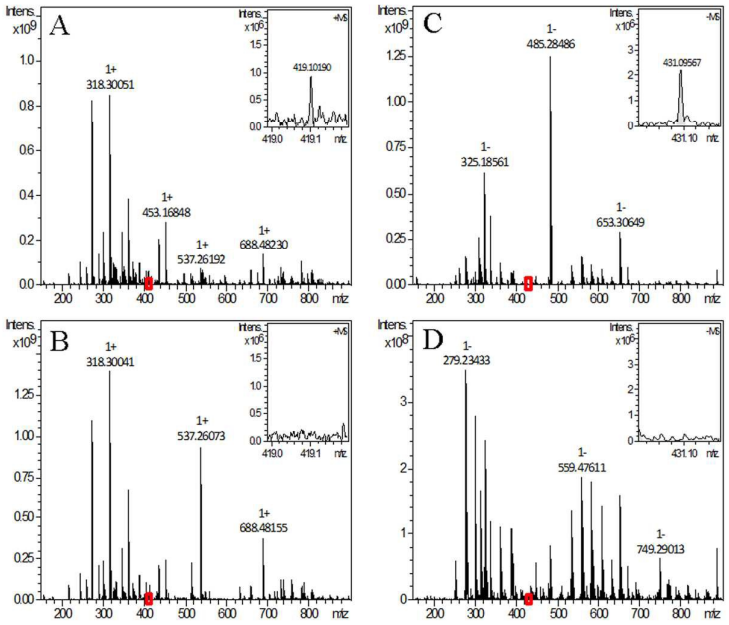

Fig. 11 ESI(-/+)-MS spectra of the extract of the tumor tissue. (A) ESI(+)-MS spectrum of the extract of the tumor tissue of S180 mice treated with 1.0 μmol/kg/day of THPDTPI for 14 days, the local amplified insert shows an ion peak of THPDTPI plus Na at 419.10190; (B) ESI(+)-MS spectrum of the extract of the tumor tissue of S180 mice treated with CMCNa for 14 days, the local amplified insert shows no such an ion peak; (C) ESI(-)-MS spectrum of the extract of the

tumor tissue of S180 mice treated with 1.0 μmol/kg/day of THPDTPI for 14 days, the local amplified insert shows an ion peak of THPDTPI plus Cl at 431.09567; (D) ESI(-)-MS spectrum of the extract of the tumor tissue of S180 mice treated with CMCNa for 14 days, the local amplified insert shows no such an ion peak.

Experimental section

The detailed methodologies for all experiments are given as ESI.†

Sprague Dawley rats and ICR mice were purchased from the Animal Center of Peking University. Work performed was based on a protocol reviewed and approved by the ethics committee of Capital Medical University. The committee assures that the welfare of the animals was maintained in accordance to the requirements of the Animal Welfare Act and in accordance to the NIH Guide for Care and Use of Laboratory Animals.

Conclusions

Docking investigation and spectrophotometric experiments support that the interaction between THPDTPI and CT DNA is π-π stacking intercalation; FT-MS spectrum and NOESY 2D 1HNMR spectrum together show that THPDTPI can form π-π stacking like dimer; Faraday-Tyndall effect and the images of TEM, SEM and AFM support that the dimers of THPDTPI can further self-assemble to form nano-particles, the *in vivo* anti-tumor assay, *in vitro* anti-proliferation assay and the acute toxicity evaluation logically support the rationality of the present design, and ensure the novel heptacyclic THPDTPI been a promising parent stock of nano-intercalotors. The present study also opens the gate to a promising area of discovering diverse nano-intercalation analogs of THPDTPI via constructing more novel heptacyclic molecules with modified β-carbolines.

Acknowledgements

The authors thank the BMSTC (Z141100002114049), TJSHG (201310025008), the Project of Construction of Innovative Teams and Teacher Career Development for Universities and Colleges Under Beijing Municipality, NSFC (81172930, 81273379, 81202412 and 81373264), Joint Research and Development of protective agents for low dose radiation injury (2014DFR30930) and the Beijing NOVA Program (XX2013039) for financial supports.

Notes and references

1. N. Perin, I. Martin-Kleiner, R. Nhili, W. Laine, M. H. David-Cordonnier, O. Vugrek, G. Karminski-Zamola, M. Kralj and M. Hranjec, *Medchemcomm*, 2013, 4, 1537-1550.
2. S. Singh, A. T. Baviskar, V. Jain, N. Mishra, U. C. Banerjee, P. V. Bharatam, K. Tikoo and M. P. S. Ishar, *Medchemcomm*, 2013, 4, 1257-1266.
3. Y. G. Ke, G. Bellot, N. V. Voigt, E. Fradkov and W. M. Shih, *Chem. Sci.*, 2012, 3, 2587-2597.
4. A. Kamal, R. Shetti, M. J. Ramaiah, P. Swapna, K. S. Reddy, A. Mallareddy, M. P. N. Rao, M. Chourasia, G. N. Sastry, A. Juvekar, S. Zingde, P. Sarma, S. Pushpavalli and M. Pal-Bhadra, *Medchemcomm*, 2011, 2, 780-788.
5. L. Liu, L. Wei, Y. F. Yang, M. Zhao, X. Y. Zhang, M. Q. Zheng, Y. J. Wang and S. Q. Peng, *Medchemcomm*, 2011, 2, 126-131.
6. Z. C. Zhang, Y. Y. Yang, D. N. Zhang, Y. Y. Wang, X. H. Qian and F. Y. Liu, *Bioorg. Med. Chem.*, 2006, 14, 6962-6970.
7. S. Miljanic, A. Dijanosic, I. Matosevic and I. Piantanida, *Vib. Spectrosc.*, 2011, 57, 23-29.
8. M. C. C. Luca, V. V. Tura and Mangalagiu, II, *Med. Hypotheses*, 2010, 75, 627-629.
9. J. Dickerhoff, F. Riechert-Krause, J. Seifert and K. Weisz, *Biochimie*, 2014, 107, 327-337.
10. N. Shankaraiah, K. P. Siraj, S. Nekkanti, V. Srinivasulu, P. Sharma, K. R. Senwar, M. Sathish, M. Vishnuvardhan, S. Ramakrishna, C. Jadala, N. Nagesh and A. Kamal, *Bioorg. Chem.*, 2015, 59, 130-139.
11. X. L. Li, Y. J. Lin, Y. K. Yuan, K. Liu and X. H. Qian, *Tetrahedron*, 2011, 67, 2299-2304.
12. B. Wilson, M. J. Fernandez, A. Lorente and K. B. Grant, *Tetrahedron*, 2008, 64, 3429-3436.
13. L. R. Ferguson and W. A. Denny, *Mutat. Res.*, 2007, 623, 14-23.
14. N. Jain, S. Francis and S. H. Friedman, *Bioorg. Med. Chem. Lett.*, 2012, 22,

4844-4848.

15. L. A. Howell, R. Gulam, A. Mueller, M. A. O'Connell and M. Searcey, *Bioorg. Med. Chem. Lett.*, 2010, 20, 6956-6959.
16. J. H. Wu, C. Y. Li, M. Zhao, W. J. Wang, Y. J. Wang and S. Q. Peng, *Bioorg. Med. Chem.*, 2010, 18, 6220-6229.
17. D. Pucci, T. Bellini, A. Crispini, I. D'Agnano, P. F. Liguori, P. Garcia-Orduna, S. Pirillo, A. Valentini and G. Zanchetta, *Medchemcomm*, 2012, 3, 462-468.
18. Z. Xiao, C. Ji, J. Shi, E. M. Pridgen, J. Frieder, J. Wu, O. C. Farokhzad, *Angew. Chem. Int. Ed. Engl.*, 2012, 47, 12023-12027.
19. Y. Du, X. Yang, W. Li, J. Wang, C. Huang, *RSC Adv.*, 2014, 4, 34830-34835.
20. J. H. Wu, G. H. Cui, M. Zhao, C. Y. Cui and S. Q. Peng, *Mol. Biosyst.*, 2007, 3, 855-861.
21. F. Wang, S. Li, Y. J. Wang, H. M. Zhu, X. Y. Zhang, M. Zhao, J. H. Wu and S. Q. Peng, *Medchemcomm*, 2015, 6, 956-962.
22. S. Li, Y. J. Wang, F. Wang, Y. N. Wang, X. Y. Zhang, M. Zhao, Q. Q. Feng, J. H. Wu, S. R. Zhao, W. Wu and S. Q. Peng, *Int. J. Nanomedicine*, 2015, 10, 5273-5292.
23. S. Poornima, S. Anbu, R. Ravishankaran, S. Sundaramoorthy, K. N. Vennila, A. A. Karande, D. Velmurugan and M. Kandaswamy, *Polyhedron*, 2013, 62, 26-36.
24. M. T. Li, J. W. Sun, J. Q. Sha, H. B. Wu, E. L. Zhang and T. Y. Zheng, *J. Mol. Struct.*, 2013, 1045, 29-34.
25. J. Rajesh, A. Gubendran, G. Rajagopal and P. Athappan, *J. Mol. Struct.*, 2012, 1010, 169-178.

Graphical Abstract

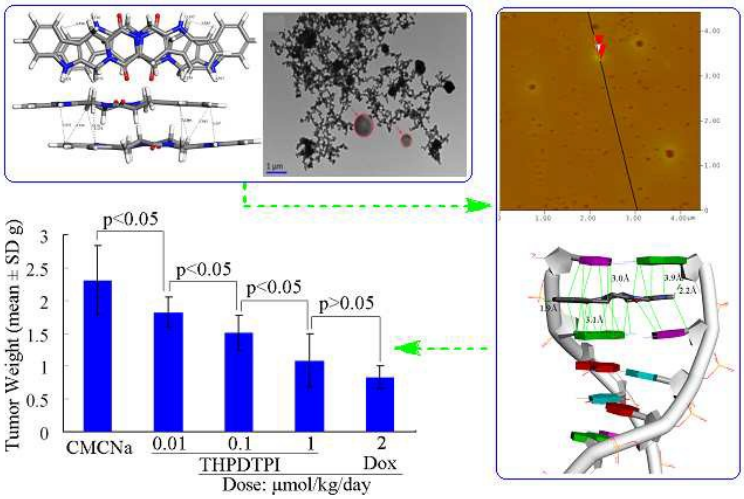

A strategy for designing safe and effective π-π stacking nano-intercalators as anti-tumor agent was presented for the first time.